Interacting Energy Components and Observational $H(z)$ Data

Hao Wei [1,*] and Shuang Nan Zhang [1,2,3]

[1] *Department of Physics and Tsinghua Center for Astrophysics, Tsinghua University, Beijing 100084, China*
[2] *Key Laboratory of Particle Astrophysics, Institute of High Energy Physics, Chinese Academy of Sciences, Beijing 100049, China*
[3] *Physics Department, University of Alabama in Huntsville, Huntsville, AL 35899, USA*

Abstract

In this note, we extend our previous work [Phys. Lett. B **644**, 7 (2007), astro-ph/0609597], and compare eleven interacting dark energy models with different couplings to the observational $H(z)$ data. However, none of these models is better than the simplest ΛCDM model. This implies that either more exotic couplings are needed in the cosmological models with interaction between dark energy and dust matter, or *there is no interaction at all*. We consider that this result is disadvantageous to the interacting dark energy models studied extensively in the literature.

PACS numbers: 95.36.+x, 98.80.Es, 98.80.-k

* email address: haowei@mail.tsinghua.edu.cn

1 Introduction

Nowadays, dark energy study has been one of the most active fields in modern cosmology [1], since the discovery of the present accelerated expansion of our universe [2, 3, 4, 5, 6, 7]. In the past years, many cosmological models are proposed to interpret this phenomenon. One of the important tasks is to confront them with observational data. The most frequent method to constrain the model parameters is fitting them to the luminosity distance

$$d_L(z) = (1+z)\int_0^z \frac{d\tilde{z}}{H(\tilde{z})}\,, \tag{1}$$

which is an integral of Hubble parameter $H \equiv \dot{a}/a$, where $a = (1+z)^{-1}$ is the scale factor (z is the redshift); a dot denotes the derivative with respect to cosmic time t. However, the integral cannot take the fine structure of $H(z)$ into consideration and then lose some important information compiled in it (this point is also noticed in e.g. [8]). Therefore, it is more rewarding to investigate the observational $H(z)$ data directly.

The observational $H(z)$ data we used here are based on differential ages of the oldest galaxies [9]. In [10], Jimenez *et al.* obtained an independent estimate for the Hubble constant by the method developed in [9], and used it to constrain the equation-of-state parameter (EoS) of dark energy. The Hubble parameter depends on the differential age as a function of redshift z in the form

$$H(z) = -\frac{1}{1+z}\frac{dz}{dt}\,. \tag{2}$$

Therefore, a determination of dz/dt directly measures $H(z)$ [11]. By using the differential ages of passively evolving galaxies determined from the Gemini Deep Deep Survey (GDDS) [12] and archival data [13], Simon *et al.* determined $H(z)$ in the range $0 \lesssim z \lesssim 1.8$ [11]. The observational $H(z)$ data from [11] are given in Table 1 and shown in Figs. 2–5.

z	0.09	0.17	0.27	0.40	0.88	1.30	1.43	1.53	1.75
$H(z)$ (km s^{-1} Mpc^{-1})	69	83	70	87	117	168	177	140	202
1σ uncertainty	$\pm$12	$\pm$8.3	$\pm$14	$\pm$17.4	$\pm$23.4	$\pm$13.4	$\pm$14.2	$\pm$14	$\pm$40.4

Table 1: The observational $H(z)$ data [10, 11] (see [14, 15] also).

These observational $H(z)$ data have been used to constrain the dark energy potential and its redshift dependence by Simon *et al.* in [11]. Yi and Zhang used them to constrain the parameters of holographic dark energy model in [16]. In [14], Samushia and Ratra have used these observational $H(z)$ data to constrain the parameters of ΛCDM, XCDM and ϕCDM models. Some relevant works also include [8, 15, 16, 17, 18, 19, 20] for examples.

By looking carefully on the observational $H(z)$ data given in Table 1 and shown in Figs. 2–5, we notice that two data points near $z \sim 1.5$ and 0.3 are very special. They deviate from the main trend and dip sharply, especially the one near $z \sim 1.5$; the $H(z)$ decreases and then increases around them. This hints that the effective EoS crossed -1 there. In our previous work [15], we have confronted ten cosmological models with observational $H(z)$ data, and found that the best models have an oscillating feature for both $H(z)$ and effective EoS, with the effective EoS crossing -1 around redshift $z \sim 1.5$, while other non-oscillating dark energy models (e.g. ΛCDM, XCDM, vector-like dark energy etc.) cannot catch the main feature of the observational $H(z)$ data.

In Fig. 1, we show the quantity $L(z) \equiv H^2(z)/H_0^2 - \Omega_{m0}(1+z)^3$ versus redshift z, which is associated with the fractional energy density of dark energy, for the fiducial parameters $H_0 = 72$ km s^{-1} Mpc^{-1} and $\Omega_{m0} = 0.3$ or 0.28, where the subscript "0" indicates the present value of the corresponding quantity. It is

easy to see that the fractional energy density of dark energy of the point near $z \sim 1.5$ is negative (beyond 1σ significance). To avoid this, one can decrease the corresponding Ω_{m0} or make the matter decrease with the expansion of our universe slower than a^{-3}. Inspired by this, it is natural to consider the possibility of exchanging energy between dark energy and dust matter through interaction. In fact, we considered the cases with constant coupling coefficient in [15]. However, we found that it is not preferred by the observational $H(z)$ data. In the present work, we will explore more forms of couplings between dark energy and dust matter, in an attempt to find the couplings which can best describe the observational $H(z)$ data.

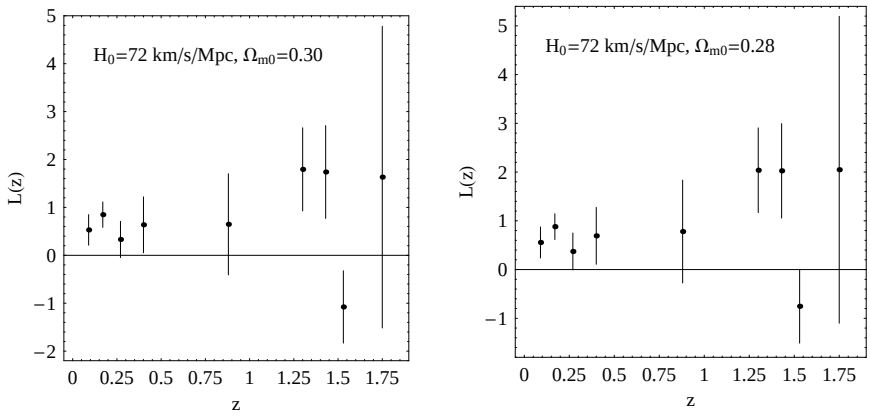

Figure 1: The quantity $L(z) \equiv H^2(z)/H_0^2 - \Omega_{m0}(1+z)^3$ versus redshift z, for the fiducial parameters $H_0 = 72$ km s^{-1} Mpc^{-1} and $\Omega_{m0} = 0.3$ (left panel) or 0.28 (right panel).

As extensively considered in the literature (see e.g. [21, 22, 23, 24, 25, 26, 27, 28, 29, 30, 31, 32, 33, 35, 36, 39, 40, 41, 42, 43]), we assume that dark energy and dust matter exchange energy through interaction according to

$$\dot{\rho}_X + 3H\left(\rho_X + p_X\right) = -3QH\rho_m, \tag{3}$$

$$\dot{\rho}_m + 3H\rho_m = 3QH\rho_m, \tag{4}$$

which preserves the total energy conservation equation $\dot{\rho}_{tot} + 3H\left(\rho_{tot} + p_{tot}\right) = 0$. We assume that the EoS of dark energy $w_X \equiv p_X/\rho_X$ is constant, and consider a spatially flat Friedmann-Robertson-Walker (FRW) universe throughout this work. Notice that the coupling coefficient $Q = Q(z)$ can be any function of redshift z. So, the interaction term $3QH\rho_m$ is a general form, in contrast to the first glance. Integrating Eq. (4), it is easy to get

$$\rho_m \propto \exp\left[\int 3(Q-1)dN\right], \tag{5}$$

where $N \equiv \ln a = -\ln(1+z)$ is the so-called e-folding time; the constant proportional coefficient can be determined by requiring $\rho_m(N=0) = \rho_{m0}$. Then, ρ_X can be also obtained by substituting ρ_m into Eq. (3). From the Friedmann equation $3H^2 = 8\pi G(\rho_m + \rho_X)$, the Hubble parameter is in hand.

In the following sections, we will compare the observational $H(z)$ data with some cosmological models with different couplings. We adopt the prior $H_0 = 72$ km s^{-1} Mpc^{-1}, which is exactly the median value of the result from the Hubble Space Telescope (HST) key project [34], and is also well consistent with the

one from WMAP 3-year result [4]. Since there are only 9 observational $H(z)$ data points and their errors are fairly large, they cannot severely constrain model parameters alone. We perform a χ^2 analysis and compare the cosmological models to find out the one which catches the main features of the observational $H(z)$ data. We determine the best-fit values for the model parameters by minimizing

$$\chi^2(parameters) = \sum_{i=1}^{9} \frac{\left[H_{mod}(parameters; z_i) - H_{obs}(z_i)\right]^2}{\sigma^2(z_i)}\,, \tag{6}$$

where H_{mod} is the predicted value for the Hubble parameter in the assumed model, H_{obs} is the observed value, σ is the corresponding 1σ uncertainty, and the summation is over the 9 observational $H(z)$ data points at redshift z_i.

2 Simple couplings

We firstly consider the simplest case, $Q = 0$, namely there is no interaction between dark energy and dust matter. It is easy to find that the Hubble parameter is given by [15]

$$H(z) = H_0\sqrt{\Omega_{m0}(1+z)^3 + (1-\Omega_{m0})(1+z)^{3(1+w_X)}}\,, \tag{7}$$

where $\Omega_{m0} \equiv 8\pi G\rho_{m0}/(3H_0^2)$ is the present fractional energy density of dust matter. By minimizing the corresponding χ^2, we find that the best-fit values for model parameters are $\Omega_{m0} = 0.28$ and $w_X = -0.90$, while $\chi^2_{min} = 9.02$ for 7 degrees of freedom and $P\left(\chi^2 > \chi^2_{min}\right) = 0.25$.

Next, we consider the case of $Q = const.$. By using Eqs. (5) and (3), we can obtain the Hubble parameter as [15]

$$H(z) = H_0\sqrt{\frac{w_X\Omega_{m0}}{Q+w_X}(1+z)^{3(1-Q)} + \left(1 - \frac{w_X\Omega_{m0}}{Q+w_X}\right)(1+z)^{3(1+w_X)}}\,. \tag{8}$$

By minimizing the corresponding χ^2, we find that the best-fit values for model parameters are $\Omega_{m0} = 0.72$, $w_X = -3.70$ and $Q = 0.30$, while $\chi^2_{min} = 8.48$ for 6 degrees of freedom and $P\left(\chi^2 > \chi^2_{min}\right) = 0.21$. Although the χ^2_{min} is reduced slightly compare to the case of $Q = 0$, statistically this fitting has no significant improvement over the case of $Q = 0$, since the number of parameters is increased from 2 to 3.

Another Q with only one parameter comes from the assumption [33, 35, 36]

$$\frac{\rho_X}{\rho_m} = \frac{\rho_{X0}}{\rho_{m0}}a^{\xi}, \tag{9}$$

where ξ is a constant parameter, which quantifies the severity of the coincidence problem. Following [33, 35, 36], it is easy to find that the corresponding Q is given by (which is labeled as SCL)

$$Q(z) = \frac{Q_0}{1 - \Omega_{m0} + \Omega_{m0}(1+z)^{\xi}}, \tag{10}$$

where $Q_0 = -(1-\Omega_{m0})(\xi + 3w_X)/3$; and the Hubble parameter reads

$$H(z) = H_0(1+z)^{3/2}\left[\Omega_{m0} + (1-\Omega_{m0})(1+z)^{-\xi}\right]^{-3w_X/(2\xi)}\,. \tag{11}$$

By minimizing the corresponding χ^2, we find that the best-fit values for model parameters are $\Omega_{m0} = 0.92$, $w_X = -8.72$ and $\xi = 1.49$, while $\chi^2_{min} = 8.88$ for 6 degrees of freedom and $P\left(\chi^2 > \chi^2_{min}\right) = 0.18$. It is worth noting that the best-fit value $\Omega_{m0} = 0.92$ is inconsistent with the results from clusters of galaxies [38] and 3-year WMAP [4] etc.

We present the observational $H(z)$ data with error bars, and the theoretical lines for these simple models with the corresponding best-fit parameters in Fig. 2. In fact, the cases of $Q = 0$ and SCL cannot be distinguished significantly. It can be seen clearly from Fig. 2 that none of them may reproduce the sharp dip around $z \sim 1.5$; the data point near $z \sim 1.5$ deviates from model fitting by about 2σ. In fact, it can be seen from Table 2, all of these models are statistically even worse than the ΛCDM model.

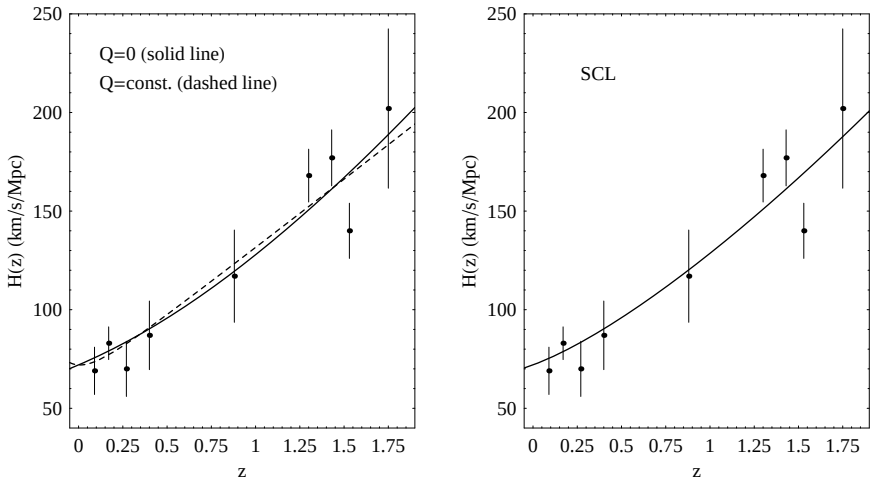

Figure 2: The observational $H(z)$ data with error bars, and the theoretical lines for three simple models with the corresponding best-fit parameters. Left panel: the cases of $Q = 0$ (solid line) and $Q = const.$ (dashed line); Right panel: the case of SCL.

3 More complicated couplings

In this section, we will consider some more complicated couplings. Unlike in Section 2, for these complicated cases, it is difficult to obtain the analytical $\rho_X(z)$ from Eq. (3) with Eq. (5), and then the Hubble parameter $H(z)$. Therefore, the numerical methods [37] are necessary. For the convenience of numerical computing, we introduce $\tilde{\rho}_m \equiv 8\pi G\rho_m/(3H_0^2)$ and $\tilde{\rho}_X \equiv 8\pi G\rho_X/(3H_0^2)$. Eqs. (3) and (5) become

$$\frac{d\tilde{\rho}_X}{dN} = -3\tilde{\rho}_X(1 + w_X) - 3Q\tilde{\rho}_m, \tag{12}$$

$$\tilde{\rho}_m \propto \exp\left[\int 3(Q-1)dN\right], \tag{13}$$

where the constant proportional coefficient in Eq. (13) is determined by requiring $\tilde{\rho}_m(N = 0) = \Omega_{m0}$; the initial condition for integrating Eq. (12) is $\tilde{\rho}_X(N = 0) = 1 - \Omega_{m0}$. The Hubble parameter is given by $H = H_0(\tilde{\rho}_X + \tilde{\rho}_m)^{1/2}$. In the following subsections, we will consider some cases with *parameterized* $Q(N)$. We restrict ourselves to the cases with only two parameters, since the data points are so few. To find the minimal χ^2 efficiently, we scan the parameters space with a relatively large grid size at first, and then narrow the parameters space and scan with a small grid size. In the procedure, we impose the condition $\tilde{\rho}_X \geq 0$, while $\tilde{\rho}_m \geq 0$ has been guaranteed by Eq. (13) for real $Q(N)$.

3.1 Linear coupling

Here, we consider a linear coupling (LIN)

$$Q(N) = Q_0 + Q_1 N, \tag{14}$$

where Q_0 and Q_1 are constants. The corresponding $\tilde{\rho}_m$ is given by

$$\tilde{\rho}_m = \Omega_{m0} \exp\left[3(Q_0 - 1)N + \frac{3}{2} Q_1 N^2\right]. \tag{15}$$

We find that the best-fit parameters are $\Omega_{m0} = 0.001$, $w_X = -0.80$, $Q_0 = -7.78$ and $Q_1 = -14.32$, while $\chi^2_{min} = 7.08$ for 5 degrees of freedom and $P\left(\chi^2 > \chi^2_{min}\right) = 0.21$.

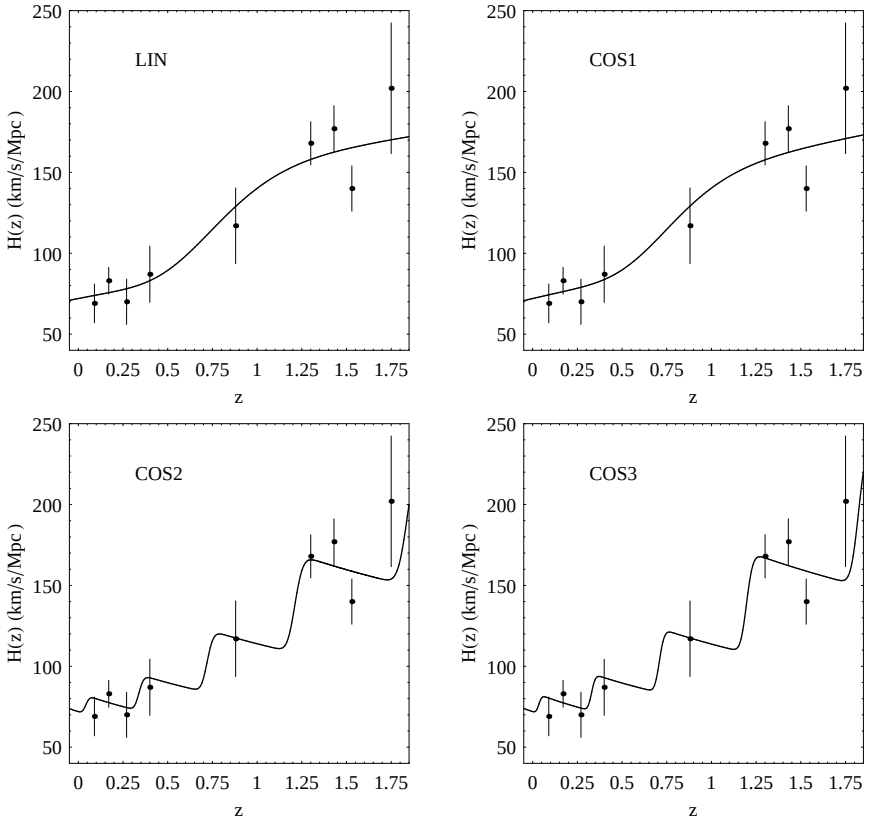

Figure 3: The observational $H(z)$ data with error bars, and the theoretical lines for the cases of LIN, COS1, COS2 and COS3, with the corresponding best-fit parameters.

3.2 Couplings of cosine type

We consider a coupling of cosine type (COS1) as

$$Q(N) = A_1 \cos(A_2 N), \tag{16}$$

where A_1 and A_2 are constants. The corresponding $\tilde{\rho}_m$ is given by

$$\tilde{\rho}_m = \Omega_{m0} \exp\left[-3N + 3\frac{A_1}{A_2}\sin\left(A_2 N\right)\right]. \tag{17}$$

We find that the best-fit parameters are $\Omega_{m0} = 0.001$, $w_X = -0.76$, $A_1 = -6.09$ and $A_2 = 2.87$, while $\chi^2_{min} = 7.07$ for 5 degrees of freedom and $P\left(\chi^2 > \chi^2_{min}\right) = 0.22$.

The next one (COS2) is given by

$$Q(N) = A_1^3 \cos\left(N/A_2 + A_1\pi\right). \tag{18}$$

It is easy to find that

$$\tilde{\rho}_m = \Omega_{m0} \exp\left\{-3N + 3A_1^3 A_2\left[\sin\left(N/A_2 + A_1\pi\right) - \sin\left(A_1\pi\right)\right]\right\}. \tag{19}$$

We find that the best-fit parameters are $\Omega_{m0} = 0.07$, $w_X = -1.33$, $A_1 = -3.83$ and $A_2 = -0.04$, while $\chi^2_{min} = 5.89$ for 5 degrees of freedom and $P\left(\chi^2 > \chi^2_{min}\right) = 0.32$.

We consider the third case (COS3)

$$Q(N) = A_1^3 \cos\left(N/A_2 + \pi/A_1\right). \tag{20}$$

The corresponding $\tilde{\rho}_m$ reads

$$\tilde{\rho}_m = \Omega_{m0} \exp\left\{-3N + 3A_1^3 A_2\left[\sin\left(N/A_2 + \pi/A_1\right) - \sin\left(\pi/A_1\right)\right]\right\}. \tag{21}$$

The best-fit parameters are found to be $\Omega_{m0} = 0.07$, $w_X = -1.35$, $A_1 = -4.41$ and $A_2 = 0.04$, while $\chi^2_{min} = 5.88$ for 5 degrees of freedom and $P\left(\chi^2 > \chi^2_{min}\right) = 0.32$.

In Fig. 3, we present the observational $H(z)$ data with error bars, and the theoretical lines for the cases of LIN, COS1, COS2 and COS3, with the corresponding best-fit parameters. It can be seen clearly from Fig. 3 that the cases of LIN and COS1 cannot reproduce the sharp dip around $z \sim 1.5$. Although the cases of COS3 and COS4 have the oscillating feature, the data points near $z \sim 1.5$ and 1.75 deviate from model fitting beyond 1σ. We notice that the best-fit parameter Ω_{m0} for the cases of LIN, COS1, COS2 and COS3 are too small to be consistent with the results from clusters of galaxies [38] and 3-year WMAP [4] etc. After all, even purely from statistical point of view, all these models are not preferred over the ΛCDM model.

3.3 Couplings of Gaussian distribution type

In this subsection, we consider some couplings of Gaussian distribution type. In fact, they can efficiently mimic the δ function, namely, these Q can be rather large in a very narrow range of N and are approximately zero for other N.

We consider the case of original Gaussian distribution (GD1) at first,

$$Q(N) = \frac{1}{\sqrt{\pi}\, Q_s} \exp\left[-\frac{(N - N_s)^2}{Q_s^2}\right], \tag{22}$$

where Q_s and N_s are constants. The corresponding $\tilde{\rho}_m$ is given by

$$\tilde{\rho}_m = \Omega_{m0} \exp\left[-3N + \frac{3}{2}\,\mathrm{Erf}\left(\frac{N - N_s}{Q_s}\right) + \frac{3}{2}\,\mathrm{Erf}\left(\frac{N_s}{Q_s}\right)\right], \tag{23}$$

where $\mathrm{Erf}(x) \equiv \dfrac{2}{\sqrt{\pi}} \displaystyle\int_0^x e^{-t^2} dt$ is the well-known error function [37]. We find that the best-fit parameters are $\Omega_{m0} = 0.43$, $w_X = -1.64$, $Q_s = 0.007$ and $N_s = -0.85$, while $\chi^2_{min} = 5.89$ for 5 degrees of freedom and $P\left(\chi^2 > \chi^2_{min}\right) = 0.32$.

Then, we consider a variant (GD2) of the original Gaussian distribution as

$$Q(N) = \frac{2}{\sqrt{\pi}\, Q_s^3} \exp\left[-\frac{(N-N_s)^2}{Q_s^2}\right], \tag{24}$$

and find that

$$\tilde{\rho}_m = \Omega_{m0} \exp\left\{-3N + \frac{3}{Q_s^2}\left[\mathrm{Erf}\left(\frac{N-N_s}{Q_s}\right) + \mathrm{Erf}\left(\frac{N_s}{Q_s}\right)\right]\right\}. \tag{25}$$

We obtain the best-fit parameters as $\Omega_{m0} = 0.43$, $w_X = -1.61$, $Q_s = 0.014$ and $N_s = -0.89$, while $\chi^2_{min} = 5.93$ for 5 degrees of freedom and $P\left(\chi^2 > \chi^2_{min}\right) = 0.31$.

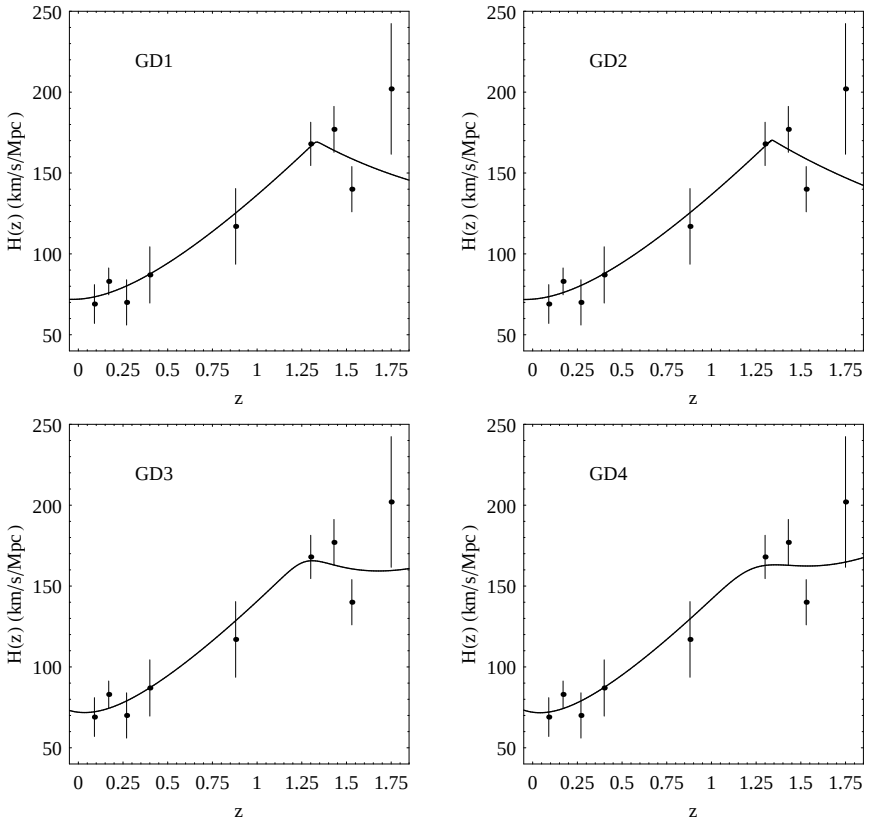

Figure 4: The observational $H(z)$ data with error bars, and the theoretical lines for the cases of GD1, GD2, GD3 and GD4, with the corresponding best-fit parameters.

Also, other variant (GD3) of the original Gaussian distribution can be the form of

$$Q(N) = \frac{2}{\sqrt{\pi}\, Q_s} \exp\left[-\frac{(N-N_s)^2}{Q_s^4}\right]. \tag{26}$$

Its corresponding $\tilde{\rho}_m$ is given by

$$\tilde{\rho}_m = \Omega_{m0} \exp\left\{-3N + 3Q_s\left[\mathrm{Erf}\left(\frac{N-N_s}{Q_s^2}\right) + \mathrm{Erf}\left(\frac{N_s}{Q_s^2}\right)\right]\right\}. \tag{27}$$

We find that the best-fit parameters are $\Omega_{m0} = 0.47$, $w_X = -2.10$, $Q_s = 0.21$ and $N_s = -0.83$, while $\chi^2_{min} = 6.07$ for 5 degrees of freedom and $P\left(\chi^2 > \chi^2_{min}\right) = 0.30$.

We consider the last one (GD4) as

$$Q(N) = \frac{2}{\sqrt{\pi}\, Q_s} \exp\left[-\frac{(N - N_s)^2}{Q_s^6}\right]. \tag{28}$$

It is easy to find that

$$\tilde{\rho}_m = \Omega_{m0} \exp\left\{-3N + 3Q_s^2\left[\mathrm{Erf}\left(\frac{N - N_s}{Q_s^3}\right) + \mathrm{Erf}\left(\frac{N_s}{Q_s^3}\right)\right]\right\}. \tag{29}$$

We obtain the best-fit parameters as $\Omega_{m0} = 0.48$, $w_X = -2.20$, $Q_s = 0.42$ and $N_s = -0.82$, while $\chi^2_{min} = 6.43$ for 5 degrees of freedom and $P\left(\chi^2 > \chi^2_{min}\right) = 0.27$.

In Fig. 4, we present the observational $H(z)$ data with error bars, and the theoretical lines for the cases of GD1, GD2, GD3 and GD4, with the corresponding best-fit parameters. It can be seen clearly from Fig. 4 that the data points near $z \sim 1.5$ and 1.75 deviate from model fitting about 1σ. Again, none of these models is better than the ΛCDM model.

4 Conclusion and discussions

In this note, we extend our previous work [15], and compare eleven interacting dark energy models with different couplings to the observational $H(z)$ data. In Table 2, we summarize all eleven models considered in this work. In addition, we show the results for the simplest ΛCDM model from [15] together. Obviously, although the χ^2_{min} of all interacting dark energy models are lower than the simplest ΛCDM model, their χ^2_{min}/dof are higher, and their $P\left(\chi^2 > \chi^2_{min}\right)$ are lower correspondingly. This implies that either more exotic couplings are needed in the cosmological models with interaction between dark energy and dust matter, or *there is no interaction at all*. We consider that this result is disadvantageous to the interacting dark energy models studied extensively in the literature (see [21, 22, 23, 24, 25, 26, 27, 28, 29, 30, 31, 32, 33, 35, 36, 39, 40, 41, 42, 43] for examples).

Although the simplest ΛCDM model looks better, however, it is not the best model which is preferred by the observational $H(z)$ data. In fact, as shown in our previous work [15], the observational $H(z)$ data favors the models which have an oscillating feature for both $H(z)$ and effective EoS, with the effective EoS crossing -1 around redshift $z \sim 1.5$. Since as shown in the present work the interacting dark energy models fail, other physical mechanisms are needed to produce an oscillating feature for $H(z)$ which can also fit the observational $H(z)$ data fairly well. We leave this to our future works.

We stress that other current data, such as SNe Ia [2, 3, 7], CMB [4] and so on, are not inconsistent with the ΛCDM model, as shown in e.g. [44]. Even for the observational $H(z)$ data, we notice that from Table 2, the ΛCDM model has $\chi^2_{min} = 9.04$ for eight degrees of freedom with 34% probability, which is not unacceptably low. Before the new and improved $H(z)$ data are available, it is too early to say that the ΛCDM model can be ruled out.

In fact, we can also consider the couplings with three parameters, such as $Q(N) = A_1 \cos(A_2 N + A_3\pi)$, $Q(N) = A_s \exp\left[-(N - N_s)^2/Q_s^2\right]$, $Q(N) = A_s \exp\left[-(N - N_s)^2/Q_s^4\right]$ and so on. However, they are less attractive, since the data points are so few. Also, in addition to the couplings of Gaussian distribution type, $Q(N)$ can mimic δ function through e.g. $Q(N) = Q_h\,\mathrm{sech}[2(N - N_h)]$, $Q(N) = Q_h\,\mathrm{sech}[2Q_h(N - N_h)]$, $Q(N) = Q_h\,\mathrm{sech}[2Q_h^2(N - N_h)]$ and so on, where $\mathrm{sech}(x) = 1/\cosh(x)$. But we do not consider these cases in this work any more, since it is expected that they are physically similar to the cases of Gaussian distribution type.

If we discard the condition $\tilde{\rho}_X \geq 0$, the fit can be improved, such as $\chi^2_{min} = 4.63$, $\chi^2_{min}/dof = 0.93$ and $P\left(\chi^2 > \chi^2_{min}\right) = 0.46$ for parameters $\Omega_{m0} = 0.02$, $w_X = -1.73$, $A_1 = 3.16$ and $A_2 = 0.03$ for the case

Model	χ^2_{min}	χ^2_{min}/dof	$P\left(\chi^2 > \chi^2_{min}\right)$
ΛCDM	9.04	1.13	0.34
$Q = 0$	9.02	1.29	0.25
$Q = const.$	8.48	1.41	0.21
SCL	8.88	1.48	0.18
LIN	7.08	1.42	0.21
COS1	7.07	1.41	0.22
COS2	5.89	1.18	0.32
COS3	5.88	1.18	0.32
GD1	5.89	1.18	0.32
GD2	5.93	1.19	0.31
GD3	6.07	1.21	0.30
GD4	6.43	1.29	0.27

Table 2: Summarizing all eleven models considered in this work. In addition, we show the results for the simplest ΛCDM model from [15] together. We have adopted $H_0 = 72$ km s^{-1} Mpc^{-1} exactly in the computations.

of COS2, while $\chi^2_{min} = 5.77$, $\chi^2_{min}/dof = 1.15$ and $P\left(\chi^2 > \chi^2_{min}\right) = 0.33$ for parameters $\Omega_{m0} = 0.57$, $w_X = -2.41$, $A_1 = 1.35$ and $A_2 = 0.09$ for the case of COS3. However, we consider that they are not physically acceptable, since their $\tilde{\rho}_X$ become negative for some intervals of redshift z.

It is worth noting that for the cases with couplings of Gaussian distribution type, careful treatment in the numerical computing is necessary. If one naively uses the Bulirsch-Stoer method or the adaptive Runge-Kutta method [37] to integrate Eq. (12) directly, misleading results can be obtained, mainly due to the δ function feature of the Gaussian distribution. For instance, one may find that $\chi^2_{min} = 1.64$, $\chi^2_{min}/dof = 0.33$ and $P\left(\chi^2 > \chi^2_{min}\right) = 0.90$ for parameters $\Omega_{m0} = 0.41$, $w_X = -1.42$, $Q_s = 0.10$ and $N_s = -0.89$ for the case of GD3. However, this is misleading. We present the corresponding results of $H(z)$ and $\tilde{\rho}_X$, $\tilde{\rho}_m$ in Fig. 5. Obviously, the unaccounted fiber-like dips are not physical results. By using a more delicate treatment in the numerical computing, the right results can be obtained, as presented in Section 3.3 and Fig. 4.

Model	χ^2_{min}	χ^2_{min}/dof	$P\left(\chi^2 > \chi^2_{min}\right)$
ΛCDM	9.03	1.29	0.25
$Q = 0$	8.88	1.48	0.18
$Q = const.$	8.48	1.70	0.13
SCL	8.81	1.76	0.12

Table 3: Summarizing the four models in which H_0 is considered as a free parameter with the prior $H_0 = 72 \pm 8$ km s^{-1} Mpc^{-1} at $1\,\sigma$ uncertainty [34].

After all, it is worth noting that we adopt the exact $H_0 = 72$ km s^{-1} Mpc^{-1} throughout this work. However, we admit that the uncertainty in H_0 should be taken into account. For instance, it is suggested that in [34] $H_0 = 72 \pm 8$ km s^{-1} Mpc^{-1} at $1\,\sigma$ uncertainty, in [45] $H_0 = 68 \pm 7$ km s^{-1} Mpc^{-1} at $2\,\sigma$ uncertainty, and in [46] $H_0 = 62.3 \pm 6.3$ km s^{-1} Mpc^{-1} at $1\,\sigma$ uncertainty. So, we should examine the effects of the uncertainty in H_0 on our conclusions. Here we consider the four simplest models studied in this work for examples. They are the models ΛCDM, $Q = 0$, $Q = const.$ and SCL. The H_0 is considered as a free parameter in these models, with the prior $H_0 = 72 \pm 8$ km s^{-1} Mpc^{-1} at $1\,\sigma$ uncertainty [34]. In

this case, the total χ^2 should be the summation of the one in Eq. (6) and $\chi^2_{H0} = (H_0 - 72)^2/8^2$. We find that the best-fit values for model parameters of ΛCDM are $\Omega_{m0} = 0.31$ and $H_0 = 71.44$ km s^{-1} Mpc^{-1}, while $\chi^2_{min} = 9.03$ for 7 degrees of freedom and $P\left(\chi^2 > \chi^2_{min}\right) = 0.25$. For model $Q = 0$, the best-fit parameters are $\Omega_{m0} = 0.18$, $w_X = -0.45$ and $H_0 = 68.53$ km s^{-1} Mpc^{-1}, while $\chi^2_{min} = 8.88$ for 6 degrees of freedom and $P\left(\chi^2 > \chi^2_{min}\right) = 0.18$. For model $Q = const.$, the best-fit parameters are $\Omega_{m0} = 0.72$, $w_X = -3.68$, $Q = 0.30$ and $H_0 = 71.88$ km s^{-1} Mpc^{-1}, while $\chi^2_{min} = 8.48$ for 5 degrees of freedom and $P\left(\chi^2 > \chi^2_{min}\right) = 0.13$. For model SCL, the best-fit parameters are $\Omega_{m0} = 0.94$, $w_X = -8.45$, $\xi = 0.88$ and $H_0 = 69.79$ km s^{-1} Mpc^{-1}, while $\chi^2_{min} = 8.81$ for 5 degrees of freedom and $P\left(\chi^2 > \chi^2_{min}\right) = 0.12$. We summarize these results in Table 3. Comparing with the corresponding results of these four models in Table 2 where H_0 is taken as 72 km s^{-1} Mpc^{-1} exactly, we find that the uncertainty in H_0 cannot significantly improve the fits. Thus, even the uncertainty in H_0 is taken into consideration, our conclusions remain unchanged.

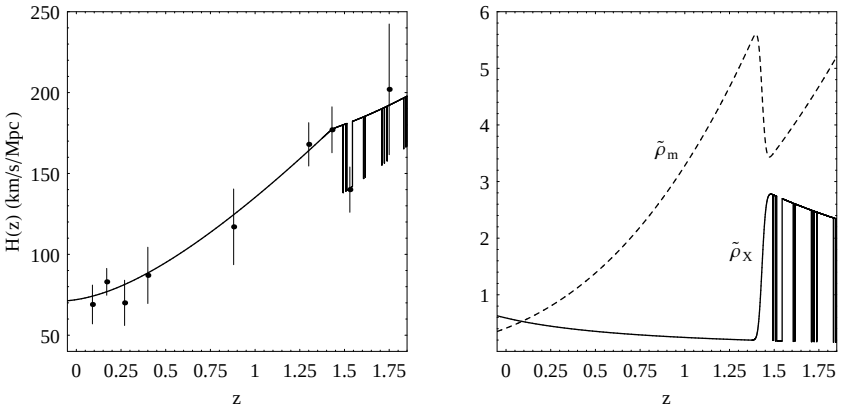

Figure 5: The numerical results for the case of GD3 with the corresponding "best-fit" parameters, which come from a careless numerical computing. See text for details.

Acknowledgments

We thank the anonymous referees for quite useful comments and suggestions, which help us to improve this work. We are grateful to Prof. Rong-Gen Cai and Prof. Zong-Hong Zhu for helpful discussions. We also thank Zong-Kuan Guo, Hongsheng Zhang, Xin Zhang, Hui Li, Meng Su and Ningning Tang, Sumin Tang, Shi-Chao Tang, Jian Hu, Yue Shen, Xin Liu, Lin Lin, Jing Jin, Wei-Ke Xiao, Feng-Yun Rao, Nan Liang, Rong-Jia Yang, Jian Wang, Yuan Liu for kind help and discussions. We acknowledge partial funding support from China Postdoctoral Science Foundation, and by the Ministry of Education of China, Directional Research Project of the Chinese Academy of Sciences under project No. KJCX2-YW-T03, and by the National Natural Science Foundation of China under project No. 10521001.

References

[1] P. J. E. Peebles and B. Ratra, Rev. Mod. Phys. **75**, 559 (2003) [astro-ph/0207347];
T. Padmanabhan, Phys. Rept. **380**, 235 (2003) [hep-th/0212290];
S. M. Carroll, astro-ph/0310342;

R. Bean, S. Carroll and M. Trodden, astro-ph/0510059;
V. Sahni and A. A. Starobinsky, Int. J. Mod. Phys. D **9**, 373 (2000) [astro-ph/9904398];
S. M. Carroll, Living Rev. Rel. **4**, 1 (2001) [astro-ph/0004075];
T. Padmanabhan, Curr. Sci. **88**, 1057 (2005) [astro-ph/0411044];
S. Weinberg, Rev. Mod. Phys. **61**, 1 (1989);
S. Nobbenhuis, Found. Phys. **36**, 613 (2006) [gr-qc/0411093];
E. J. Copeland, M. Sami and S. Tsujikawa, Int. J. Mod. Phys. D **15**, 1753 (2006) [hep-th/0603057];
R. Trotta and R. Bower, astro-ph/0607066;
A. Albrecht *et al.*, astro-ph/0609591.

[2] A. G. Riess *et al.* [Supernova Search Team Collaboration], Astron. J. **116**, 1009 (1998) [astro-ph/9805201];
S. Perlmutter *et al.* [Supernova Cosmology Project Collaboration], Astrophys. J. **517**, 565 (1999) [astro-ph/9812133];
J. L. Tonry *et al.* [Supernova Search Team Collaboration], Astrophys. J. **594**, 1 (2003) [astro-ph/0305008];
R. A. Knop *et al.*, [Supernova Cosmology Project Collaboration], Astrophys. J. **598**, 102 (2003) [astro-ph/0309368];
A. G. Riess *et al.* [Supernova Search Team Collaboration], Astrophys. J. **607**, 665 (2004) [astro-ph/0402512].

[3] P. Astier *et al.* [SNLS Collaboration], Astron. Astrophys. **447**, 31 (2006) [astro-ph/0510447];
J. D. Neill *et al.* [SNLS Collaboration], astro-ph/0605148.

[4] C. L. Bennett *et al.* [WMAP Collaboration], Astrophys. J. Suppl. **148**, 1 (2003) [astro-ph/0302207];
D. N. Spergel *et al.* [WMAP Collaboration], Astrophys. J. Suppl. **148** 175 (2003) [astro-ph/0302209];
D. N. Spergel *et al.* [WMAP Collaboration], astro-ph/0603449;
L. Page *et al.* [WMAP Collaboration], astro-ph/0603450;
G. Hinshaw *et al.* [WMAP Collaboration], astro-ph/0603451;
N. Jarosik *et al.* [WMAP Collaboration], astro-ph/0603452.

[5] M. Tegmark *et al.* [SDSS Collaboration], Phys. Rev. D **69**, 103501 (2004) [astro-ph/0310723];
M. Tegmark *et al.* [SDSS Collaboration], Astrophys. J. **606**, 702 (2004) [astro-ph/0310725];
U. Seljak *et al.*, Phys. Rev. D **71**, 103515 (2005) [astro-ph/0407372];
J. K. Adelman-McCarthy *et al.* [SDSS Collaboration], Astrophys. J. Suppl. **162**, 38 (2006) [astro-ph/0507711];
K. Abazajian *et al.* [SDSS Collaboration], astro-ph/0410239; astro-ph/0403325; astro-ph/0305492;
M. Tegmark *et al.* [SDSS Collaboration], astro-ph/0608632.

[6] S. W. Allen, R. W. Schmidt, H. Ebeling, A. C. Fabian and L. van Speybroeck, Mon. Not. Roy. Astron. Soc. **353**, 457 (2004) [astro-ph/0405340].

[7] W. M. Wood-Vasey *et al.* [ESSENCE Collaboration], astro-ph/0701041;
G. Miknaitis *et al.* [ESSENCE Collaboration], astro-ph/0701043.

[8] H. S. Zhang and Z. H. Zhu, astro-ph/0703245.

[9] R. Jimenez and A. Loeb, Astrophys. J. **573**, 37 (2002) [astro-ph/0106145].

[10] R. Jimenez, L. Verde, T. Treu and D. Stern, Astrophys. J. **593**, 622 (2003) [astro-ph/0302560].

[11] J. Simon, L. Verde and R. Jimenez, Phys. Rev. D **71**, 123001 (2005) [astro-ph/0412269].

[12] R. G. Abraham *et al.* [GDDS Collaboration], Astron. J. **127**, 2455 (2004) [astro-ph/0402436].

[13] T. Treu, M. Stiavelli, S. Casertano, P. Moller and G. Bertin, Mon. Not. Roy. Astron. Soc. **308**, 1037 (1999);
T. Treu, M. Stiavelli, P. Moller, S. Casertano and G. Bertin, Mon. Not. Roy. Astron. Soc. **326**, 221 (2001) [astro-ph/0104177];
T. Treu, M. Stiavelli, S. Casertano, P. Moller and G. Bertin, Astrophys. J. Lett. **564**, L13 (2002);
J. Dunlop, J. Peacock, H. Spinrad, A. Dey, R. Jimenez, D. Stern and R. Windhorst, Nature **381**, 581 (1996);
H. Spinrad, A. Dey, D. Stern, J. Dunlop, J. Peacock, R. Jimenez and R. Windhorst, Astrophys. J. **484**, 581 (1997);
L. A. Nolan, J. S. Dunlop, R. Jimenez and A. F. Heavens, Mon. Not. Roy. Astron. Soc. **341**, 464 (2003) [astro-ph/0103450].

[14] L. Samushia and B. Ratra, Astrophys. J. **650**, L5 (2006) [astro-ph/0607301].

[15] H. Wei and S. N. Zhang, Phys. Lett. B **644**, 7 (2007) [astro-ph/0609597].

[16] Z. L. Yi and T. J. Zhang, Mod. Phys. Lett. A **22**, 41 (2007) [astro-ph/0605596].

[17] A. Kurek and M. Szydlowski, astro-ph/0702484;
R. Lazkoz and E. Majerotto, arXiv:0704.2606 [astro-ph].

[18] P. X. Wu and H. W. Yu, Phys. Lett. B **644**, 16 (2007) [gr-qc/0612055];
P. X. Wu and H. W. Yu, JCAP **0703**, 015 (2007) [astro-ph/0701446].

[19] A. A. Sen and R. J. Scherrer, astro-ph/0703416.

[20] L. I. Xu, C. W. Zhang, B. R. Chang and H. Y. Liu, astro-ph/0701519.

[21] H. Wei and R. G. Cai, Phys. Rev. D **73**, 083002 (2006) [astro-ph/0603052].

[22] H. Wei, R. G. Cai and D. F. Zeng, Class. Quant. Grav. **22**, 3189 (2005) [hep-th/0501160];
H. Wei and R. G. Cai, Phys. Rev. D **72**, 123507 (2005) [astro-ph/0509328];
M. Alimohammadi and H. Mohseni Sadjadi, Phys. Rev. D **73**, 083527 (2006) [hep-th/0602268];
W. Zhao and Y. Zhang, Phys. Rev. D **73**, 123509 (2006) [astro-ph/0604460].

[23] A. A. Coley, gr-qc/9910074;
J. Wainwright and G. F. R. Ellis, *Dynamical Systems in Cosmology*, Cambridge Univ. Press, Cambridge, 1997;
A. A. Coley, *Dynamical Systems and Cosmology*, in Series: Astrophysics and Space Science Library, Vol. 291, Springer, 2004.

[24] E. J. Copeland, A. R. Liddle and D. Wands, Phys. Rev. D **57**, 4686 (1998) [gr-qc/9711068].

[25] L. Amendola, Phys. Rev. D **60**, 043501 (1999) [astro-ph/9904120];
L. Amendola, Phys. Rev. D **62**, 043511 (2000) [astro-ph/9908023];
L. Amendola and C. Quercellini, Phys. Rev. D **68**, 023514 (2003) [astro-ph/0303228];
L. Amendola and D. Tocchini-Valentini, Phys. Rev. D **64**, 043509 (2001) [astro-ph/0011243];
L. Amendola and D. Tocchini-Valentini, Phys. Rev. D **66**, 043528 (2002) [astro-ph/0111535];
L. Amendola, C. Quercellini, D. Tocchini-Valentini and A. Pasqui, Astrophys. J. **583**, L53 (2003) [astro-ph/0205097].

[26] Z. K. Guo, R. G. Cai and Y. Z. Zhang, JCAP **0505**, 002 (2005) [astro-ph/0412624];
Z. K. Guo and Y. Z. Zhang, Phys. Rev. D **71**, 023501 (2005) [astro-ph/0411524].

[27] T. Damour and A. M. Polyakov, Nucl. Phys. B **423**, 532 (1994) [hep-th/9401069];
T. Damour and A. M. Polyakov, Gen. Rel. Grav. **26**, 1171 (1994) [gr-qc/9411069];
C. Wetterich, Astron. Astrophys. **301**, 321 (1995) [hep-th/9408025];
J. R. Ellis, S. Kalara, K. A. Olive and C. Wetterich, Phys. Lett. B **228**, 264 (1989);
G. Huey, P. J. Steinhardt, B. A. Ovrut and D. Waldram, Phys. Lett. B **476**, 379 (2000) [hep-th/0001112];
C. T. Hill and G. G. Ross, Nucl. Phys. B **311**, 253 (1988);
G. W. Anderson and S. M. Carroll, astro-ph/9711288;
B. Gumjudpai, T. Naskar, M. Sami and S. Tsujikawa, JCAP **0506**, 007 (2005) [hep-th/0502191].

[28] H. Wei and R. G. Cai, Phys. Rev. D **71**, 043504 (2005) [hep-th/0412045].

[29] H. Wei and R. G. Cai, astro-ph/0607064.

[30] W. Zimdahl, D. Pavon and L. P. Chimento, Phys. Lett. B **521**, 133 (2001) [astro-ph/0105479];
L. P. Chimento, A. S. Jakubi, D. Pavon and W. Zimdahl, Phys. Rev. D **67**, 083513 (2003) [astro-ph/0303145].

[31] R. G. Cai and A. Wang, JCAP **0503**, 002 (2005) [hep-th/0411025];
E. Majerotto, D. Sapone and L. Amendola, astro-ph/0410543.

[32] M. Szydlowski, Phys. Lett. B **632**, 1 (2006) [astro-ph/0502034];
M. Szydlowski, T. Stachowiak and R. Wojtak, Phys. Rev. D **73**, 063516 (2006) [astro-ph/0511650].

[33] Z. K. G. Guo, N. Ohta and S. Tsujikawa, astro-ph/0702015.

[34] W. L. Freedman *et al.*, Astrophys. J. **553**, 47 (2001) [astro-ph/0012376].

[35] N. Dalal, K. Abazajian, E. Jenkins and A. V. Manohar, Phys. Rev. Lett. **87**, 141302 (2001) [astro-ph/0105317].

[36] O. Bertolami, F. Gil Pedro and M. Le Delliou, astro-ph/0703462.

[37] W. H. Press *et al.*, Numerical Recipes in Fortran: The Art of Scientific Computing, Second edition, Cambridge University Press, 1997.

[38] For examples, S. Borgani, astro-ph/0605575;
S. Borgani *et al.*, Astrophys. J. **561**, 13 (2001) [astro-ph/0106428];
J. P. Henry, Astrophys. J. **609**, 603 (2004) [astro-ph/0404142].

[39] M. R. Setare, Phys. Lett. B **642**, 1 (2006) [hep-th/0609069];
M. R. Setare, Phys. Lett. B **642**, 421 (2006) [hep-th/0609104];
M. R. Setare, JCAP **0701**, 023 (2007) [hep-th/0701242].

[40] X. Zhang, Phys. Lett. B **611**, 1 (2005) [astro-ph/0503075];
X. Zhang, Mod. Phys. Lett. A **20**, 2575 (2005) [astro-ph/0503072];
X. Zhang, F. Q. Wu and J. Zhang, JCAP **0601**, 003 (2006) [astro-ph/0411221].

[41] E. Elizalde, S. Nojiri, S. D. Odintsov and P. Wang, Phys. Rev. D **71**, 103504 (2005) [hep-th/0502082];
S. Nojiri and S. D. Odintsov, Phys. Rev. D **72**, 023003 (2005) [hep-th/0505215].

[42] A. W. Brookfield, C. van de Bruck, D. F. Mota and D. Tocchini-Valentini, Phys. Rev. Lett. **96**, 061301 (2006) [astro-ph/0503349];
M. Manera and D. F. Mota, Mon. Not. Roy. Astron. Soc. **371**, 1373 (2006) [astro-ph/0504519].

[43] S. Lee, G. C. Liu and K. W. Ng, Phys. Rev. D **73**, 083516 (2006) [astro-ph/0601333].

[44] H. K. Jassal, J. S. Bagla and T. Padmanabhan, astro-ph/0601389;
K. M. Wilson, G. Chen and B. Ratra, Mod. Phys. Lett. A **21**, 2197 (2006) [astro-ph/0602321];
T. M. Davis *et al.*, astro-ph/0701510.

[45] J. R. I. Gott, M. S. Vogeley, S. Podariu and B. Ratra, Astrophys. J. **549**, 1 (2001) [astro-ph/0006103];
G. Chen, J. R. I. Gott and B. Ratra, Publ. Astron. Soc. Pac. **115**, 1269 (2003) [astro-ph/0308099].

[46] A. Sandage, G. A. Tammann, A. Saha, B. Reindl, F. D. Macchetto and N. Panagia, Astrophys. J. **653**, 843 (2006) [astro-ph/0603647].